J Solid State Electrochem (2012) 16:3037–3043
DOI 10.1007/s10008-012-1738-z

ORIGINAL PAPER

Rubbery copolymer electrolytes containing polymerized ionic liquid for dye-sensitized solar cells

Won Seok Chi · Sung Hoon Ahn · Harim Jeon · Yong Gun Shul · Jong Hak Kim

Received: 11 December 2011 / Revised: 25 January 2012 / Accepted: 27 March 2012 / Published online: 22 April 2012

Abstract A novel type of random copolymer comprised of a polymerized ionic liquid, poly(1-((4-ethenylphenyl)methyl)-3-butyl-imidazolium iodide) (PEBII), and amorphous rubbery poly(oxyethylene methacrylate) (POEM) was synthesized and employed as a solid electrolyte in an I_2-free dye-sensitized solar cell (DSSC). The copolymer electrolytes deeply infiltrated into the nanopores of mesoporous TiO2 films, resulting in improved interfacial contact of electrode/electrolyte. The glass transition temperature (T_g) of the PEBII–POEM (−23 °C) was lower than that of PEBII homopolymer (−4 °C), indicating greater chain flexibility in the former. However, the DSSC efficiency of PEBII–POEM (4.5 % at 100 mW/cm^2) was lower than that of PEBII (5.9 %), indicating that ion concentration is more important than chain flexibility. Interestingly, upon the introduction of ionic liquid, i.e., 1-methyl-3 propylimidazolium iodide, the efficiency of PEBII remained almost constant (5.8 %), whereas that of PEBII–POEM was significantly improved up to 7.0 % due to increased I^- ion concentration, which is one of the highest values for I_2-free DSSCs.

Keywords Dye-sensitized solar cell (DSSC) · Polymerized ionic liquid · TiO2 · Iodine-free · Polymer electrolyte

Introduction

Dye-sensitized solar cells (DSSCs), introduced by Gratzel in 1991, are one of the most promising photovoltaic technologies due to their high energy conversion efficiency (~11 %) and low cost [1]. The performance of DSSCs is strongly influenced by the dye, nanocrystalline TiO_2 layer, counterelectrode, transparent conducting oxide, substrate, or electrolyte [2–4]. DSSCs using liquid electrolyte as a I^-/I_3^- redox couple have shown a high energy conversion efficiency close to 11 % at AM1.5. However, liquid electrolyte-based DSSCs suffer from potential problems such as solvent evaporation, electrolyte leakage, and instability at high temperatures. Thus, solid-state or quasi-solid-state DSSCs have been investigated to replace conventional liquid electrolytes [5–8].

The presence of I_2 in the cell often leads to deterioration of durability and photocurrent, which is caused by the sublimation of I_2 and its incident light absorption. Furthermore, I_2 can play a role as an oxidizing agent to corrode novel metals such as grid metal Ag and Pt on the counterelectrode. These findings have sparked research in I_2-free solid-state DSSCs (ssDSSCs) using a conducting polymer or a polymerized ionic liquid [9–17]. Our group recently reported I_2-free ssDSSCs based on a solid-state polymerized conducting polymer, i.e., poly(2,5-dibromo-3,4-ethylenedioxythiophene) [18], or a polymerized ionic liquid, i.e., poly((1-(4-ethenylphenyl)methyl)-3-butyl-imidazolium iodide) (PEBII) [19], that can sufficiently penetrate the TiO_2 nanopores. These ssDSSCs exhibited cell efficiencies of 5.4 and 5.9 %, respectively.

Poly(ethylene oxide) (PEO) has long been a favorable candidate as a host polymer to dissolve various metal salts and ionic liquid. However, the ionic conductivity of PEO-based electrolytes is often limited due to crystalline formation. Poly(oxyethylene methacrylate) (POEM) is a representative amorphous PEO which has high ionic conductivity but poor mechanical properties. Thus, we describe here a new type of copolymer consisting of PEBII containing iodine ions and amorphous rubbery POEM having good

W. S. Chi · S. H. Ahn · H. Jeon · Y. G. Shul · J. H. Kim (✉)
Department of Chemical and Biomolecular Engineering,
Yonsei University,
262 Seongsanno, Seodaemun-gu,
Seoul 120-749, South Korea
e-mail: jonghak@yonsei.ac.kr

compatibility with the hydrophilic ionic liquids. The materials were characterized using ^{1}H-nuclear magnetic resonance (^{1}H-NMR), Fourier transform-infrared (FT-IR) spectroscopy, differential scanning calorimetry (DSC), and ultraviolet (UV)-visible spectroscopy. The performances of DSSCs fabricated with PEBII–POEM polymer electrolytes with and without an ionic liquid, i.e., 1-methyl-3 propylimidazolium iodide (MPII), were reported here. Interfacial properties between the electrodes and the electrolyte were also characterized in detail using electrochemical impedance spectroscopy (EIS) and field emission scanning electron microscopy (FE-SEM).

Experimental

Materials

Various chemicals including 1-butylimidazole, 4-vinylbenzyl chloride, lithium iodide (LiI), acetonitirile (CH_3CN), ethyl acetate (EtOAc), poly(oxyethylene methacrylate) (POEM, poly(ethylene glycol) methyl ether methacrylate, M_n= 475 g/mol), 2,2′-azobisisobutyronitrile (AIBN), and 1-methyl-3 propylimidazolium iodide (MPII) were purchased from Aldrich and were used as received without further purification.

Synthesis of PEBII–POEM copolymer

First, a monomer, EBII, was synthesized as shown in Scheme 1, according to our previously reported method [19]. The two monomers EBII (2 g) and POEM (2 g) were dissolved in 8 ml of acetonitrile, followed by the addition of 40 ml of AIBN. A tube containing the monomers was tightly sealed, purged with nitrogen gas, and immersed in an oil bath at 60 °C for 32 h for complete polymerization. The resulting solution was precipitated in diethyl ether. The final product was dried in a vacuum oven overnight.

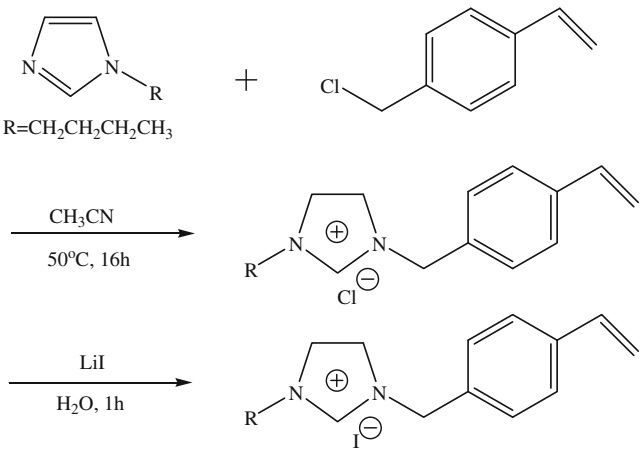

Scheme 1 Synthesis of EBII monomer

Fabrication of DSSCs

DSSCs with an active area of 0.4 cm^2 were constructed by drop-casting of electrolyte solution onto the photoelectrode and covering with the counter electrode, according to a previously reported procedure [18–21]. In order to prepare photoelectrodes, conductive F-doped tin oxide (FTO) glasses were first coated with a 75 wt% solution of titanium diisopropoxide bis(acetylacetonate) in 2-propanol. After drying at 50 °C for 30 min, the photoelectrodes were heated at 450 °C for 30 min, followed by cooling to room temperature for 8 h. A sol–gel solution containing the poly(vinyl chloride)-g-poly(oxyethylene methacrylate) (PVC-g-POEM) graft copolymer, titanium(IV) isopropoxide (TTIP), H_2O, and HCl was spin-coated onto the FTO glass and sintered at 450 °C for 30 min [20]. Then commercialized TiO_2 paste (Ti-Nanoxide T, Solaronix) was cast onto the organized mesoporous TiO_2 thin film-coated FTO glass using a doctor-blade technique, followed by sintering at 450 °C for 30 min. The TiO_2 films were functionalized overnight by the adsorption of a $Ru(dcbpy)_2(NCS)_2$ dye solution (535-bisTBA, Solaronix). Pt-layered counter electrodes were prepared by spin-coating a 1 wt% H_2PtCl_6 solution in isopropanol onto the FTO glass and then sintering at 450 °C for 30 min. A PEBII or PEBII–POEM polymer solution with or without MPII (2 and 10 wt% in acetonitrile) was directly cast onto the photoelectrode and then covered with a counter electrode. The concentration of MPII was fixed at 30 wt% with respect to the polymer. The cells were placed in a drying oven at 40 °C for 24 h and then in a vacuum oven at 40 °C for 24 h to ensure complete solvent evaporation.

Photoelectrochemical performance characteristics including the short-circuit current (J_{sc}, mA/cm^2), open-circuit voltage (V_{oc}, V), fill factor (FF), and overall energy conversion efficiency (η) were measured using a Keithley Model 2400 and a 1,000 W xenon lamp (Oriel, 91193). The light was homogeneous up to an 8×8-in.^{2} area, and its intensity was calibrated with a Si solar cell (Fraunhofer Institute for Solar Energy System, Mono-Si + KG filter, certificate no. C-ISE269) to a sunlight intensity of one (100 mW/cm^2). This calibration was confirmed with a NREL-calibrated Si solar cell (PV Measurements Inc.). The photoelectrochemical performances were calculated using the following equations:

$$\mathrm{FF} = \frac{V_{\max} \cdot J_{\max}}{V_{oc} \cdot J_{sc}} \tag{1}$$

$$\eta\,(\%) = \frac{V_{\max} \cdot J_{\max}}{P_{in}} \times 100 = \frac{V_{oc} \cdot J_{sc} \cdot \mathrm{FF}}{P_{in}} \times 100 \tag{2}$$

where J_{sc} is the short-circuit current density (milliamperes per square centimeter), V_{oc} is the open-circuit voltage (Volts), P_{in} is the incident light power, and J_{max} (milliamperes per square

centimeter), and V_{max} (Volts) are the current density and voltage in the *J–V* curve, respectively, at a maximum power output.

Characterization

^{1}H-NMR measurements were performed with a 600-MHz, high-resolution NMR spectrometer (AVANCE 600 MHz FT-NMR, Germany, Bruker). FT-IR spectra were collected using an Excalibur Series FT-IR (DIGLAB Co.) instrument between a frequency range of 4,000 and 400 cm^{-1} using ATR. DSC (2920, TA Instruments, Inc.) was used to characterize the materials at a heating rate of 10 °C/min under a N_2 environment. Ionic conductivity was measured using a two-probe method (ZAHNER IM-6 impedance analyzer) in the frequency range 1 Hz–1 MHz at room temperature. The conductivity value was calculated from the bulk electrolyte resistance value found in the complex impedance. UV-visible spectroscopy was performed with a spectrophotometer (Shimadzu) in the range of 300 to 800 nm. Morphologies of the mesoporous TiO_2 films were observed using a FE-SEM (SUPRA 55VP, Germany, Carl Zeiss).

Results and discussion

Figure 1a shows the FT-IR spectra of monomers for the synthesis of ionic liquid monomer, i.e., EBII from 1-butylimidazole. The sharp peak near 1,560 cm^{-1} is attributed to the C = N stretching vibration of the imidazole ring. A weak absorption band was also observed at 3,049 cm^{-1} resulting from the C–H aromatic bond and at 1,630 cm^{-1} due to the vinyl group of the ionic liquid. After the ion-exchange of Cl^- ions to I^- ions, the resulting EBII was more hygroscopic and viscous than the EBICl monomer.

The copolymerization of EBII and POEM via free radical reaction is illustrated in Scheme 2. The FT-IR spectra of pristine EBII, POEM, PEBII, and PEBII–POEM copolymer are presented in Fig. 1b. Upon polymerization, the weak absorption band at 1,560 cm^{-1} was observed due to the C = N stretching vibration of the imidazole ring from the EBII. The sharp absorption bands resulting from the stretching vibration modes of carbonyl (C = O) and ether bonds (C–O–C) in PEBII–POEM were observed at 1,725 and 1,096 cm^{-1}, which were shifted from the 1,717 and 1,101 cm^{-1} observed in pristine POEM. These peak shifts ware attributed to loss of π conjugation in the POEM monomer [22]. The weak absorption band at 1,638 cm^{-1} in POEM, assigned to the C = C stretching mode, completely disappeared in the PEBII–POEM, indicating successful copolymerization.

The successful copolymerization of PEBII–POEM has also been confirmed using ^{1}H NMR spectroscopy. The ^{1}H NMR spectra for PEBII and PEBII–POEM copolymers are shown in Fig. 2. The peak around 7.8 ppm is attributed to the H bonding in the imidazole ring, whereas the strong peak at 3.3 ppm is from the water adsorbed in the polymer. Upon graft copolymerization of PEBII with POEM, two peaks were additionally observed at 3.5 and 3.2 ppm, resulting from the ethylene oxide group and methyl group of POEM side chains. The composition of PEBII–POEM copolymer was calculated by comparing integral areas of peak (a) with peak (b) or (c). As a result, the composition was determined to be PEBII–POEM = 48:52 wt%, indicating its equal composition proportions based on mass.

The PEBII homopolymer showed high ionic conductivity (2.0×10^{-4} S/cm at 25 °C) due to well-aligned π-π stacking of the benzene groups, which produces a strong interaction, and proper chain length of the ionic liquid. Interestingly, the

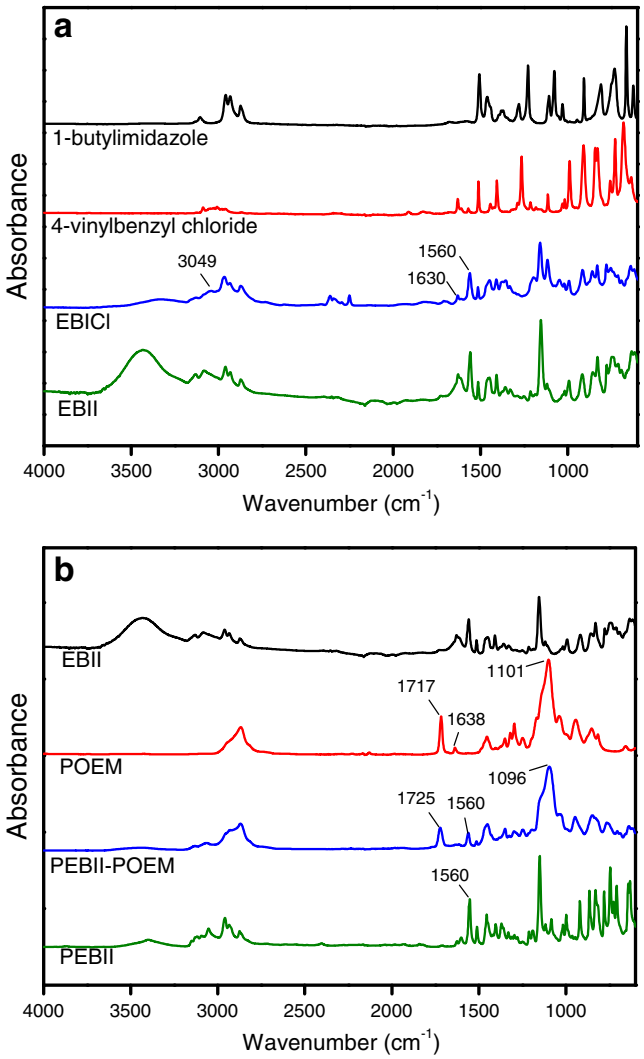

Fig. 1 FT-IR spectra **a** 1-butylimidazole, 4-vinylbenzyl chloride, 1-[(4-ethenylphenyl)methyl]-3-butyl-imidazolium chloride (EBICl) and 1-[(4-ethenylphenyl)methyl]-3-butyl-imidazolium iodide (EBII), **b** EBII and POEM monomer, PEBII and PEBII–POEM copolymer

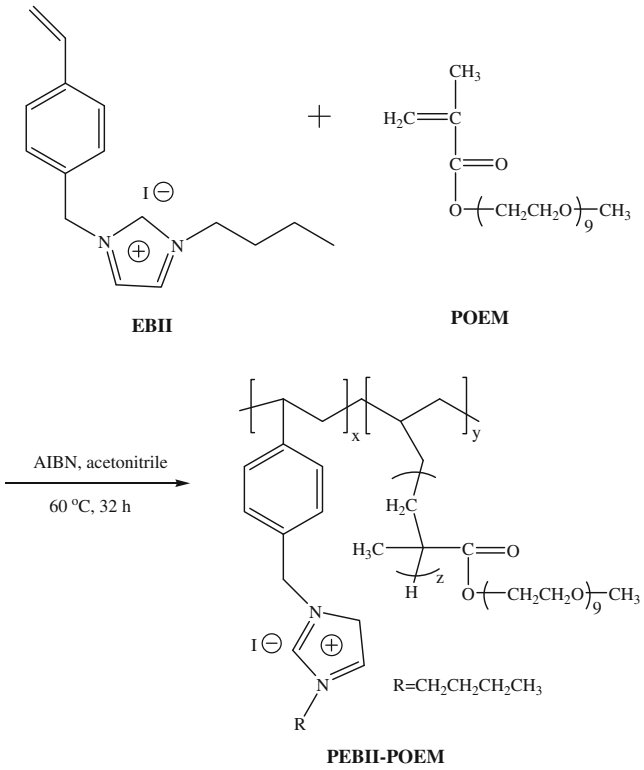

Scheme 2 Synthesis of PEBII–POEM copolymer

PEBII–POEM copolymer (2.2×10^{-4} S/cm at 25 °C) showed an ionic conductivity similar to that of the PEBII homopolymer. It is well-known that the ionic conductivities of polymer electrolytes increase with the concentration of mobile-free ions and the flexibility of polymer chains [23, 24]. PEBII has a higher ion concentration than PEBII–POEM copolymer because ions are directly dangling from PEBII chains. According to the DSC analysis in Fig. 3, however,

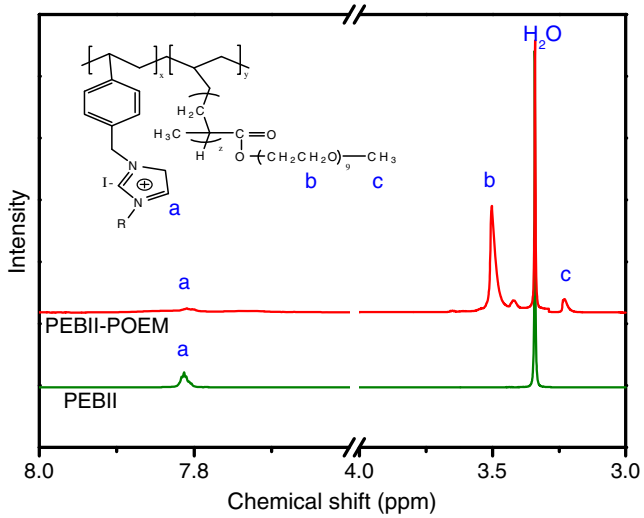

Fig. 2 ^{1}H NMR spectra for PEBII and PEBII–POEM polymers

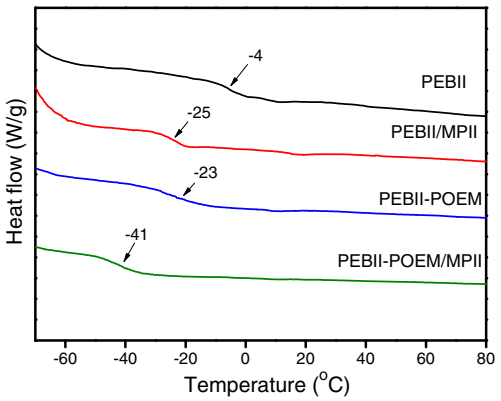

Fig. 3 DSC data for PEBII, PEBII/MPII, PEBII–POEM, and PEBII–POEM/MPII

the glass transition temperature (T_g) of PEBII was −4 °C, which was higher than the T_g (−23 °C) of PEBII–POEM due to the rubbery nature of the POEM chains. Thus, the chain flexibility of PEBII–POEM copolymer is greater than that of PEBII homopolymer. As such, a lower ion concentration of PEBII–POEM could be compensated for by greater chain flexibility. Thus, the overall ionic conductivities between the two systems were not significantly different. Upon the introduction of MPII as an ionic liquid, the T_gs of PEBII and PEBII–POEM systems decreased to −25 and −41 °C, respectively, due to plasticization of polymers by MPII.

The UV-visible spectra of PEBII, PEBII/MPII, PEBII–POEM, and PEBII–POEM/MPII mixtures are shown in Fig. 4. PEBII exhibited a strong absorption band at 370 nm and a weak shoulder band around 580 nm, attributed to the π-π* transition in the polymer main chains [25]. Upon the introduction of MPII, the band at 370 nm was not significantly changed, indicating negligible effect of MPII addition on the π-π* transition in PEBII. The intensity of the band at 370 nm was reduced in PEBII–POEM

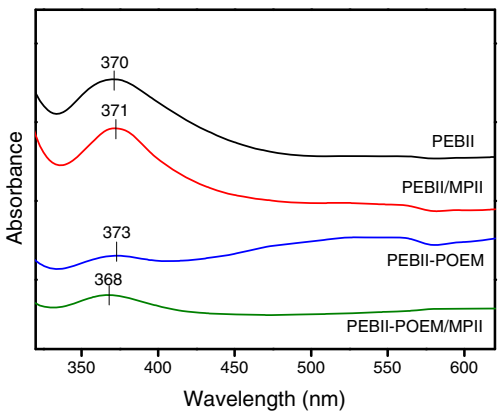

Fig. 4 UV–vis spectra for (a) PEBII, (b) PEBII/MPII, (c) PEBII–POEM, and (d) PEBII–POEM/MPII

copolymer or PEBII–POEM/MPII due to reduced content of PEBII. Furthermore, the band at 370 nm was slightly shifted, indicating some interactions between the ethylene oxide groups of POEM and the imidazolium groups of PEBII, consistent with the FT-IR results.

The infiltration of large molecular weight polymer into the TiO_2 nanopores directly affects the interfacial contact between electrolyte and electrodes, which plays a pivotal role in determining the overall conversion efficiency of solid-state DSSCs [18–21]. Thus, the surface and cross-sectional morphologies of mesoporous TiO_2 layers before and after electrolyte casting were observed using FE-SEM, as shown in Figs. 5 and 6. The mesoporous TiO_2 layer without electrolyte consisted of small nanoparticles 30–40 nm in size and large nanoparticles 100–200 nm in size, which should be the optimum structure for enhancing both surface area and light scattering. Upon introduction of polymer electrolyte, however, the morphology of the mesoporous TiO_2 layer was significantly changed. The surface of the mesoporous TiO_2 layer became much smoother due to the interconnection of TiO_2 nanoparticles resulting from adequate coating by electrolytes. The cross-sectional FE-SEM image in Fig. 6b reveals that polymer electrolyte was able to deeply penetrate the nanopores of a 10-μm-thick mesoporous TiO_2 film. For better pore filling, the size of polymer coil should be smaller than the TiO_2 nanopores [18–20]. The coil size of a polymer is commonly represented by the radius of gyration (R_g) and calculated by $R_g = C\,(M_w)^{1/2}$, where M_w (grams per mole) is the molecular weight of the polymer, and C is a constant depending on the properties of the solvent. The synthesized polymers showed M_w of 10,000–20,000 g/mol corresponding to the R_g values of 6–7 nm, which were smaller than the TiO_2 pores (10–20 nm in size). Thus, the polymer electrolytes were able to deeply infiltrate into the TiO_2 nanopores, resulting in improved interfacial contact of electrode/electrolyte.

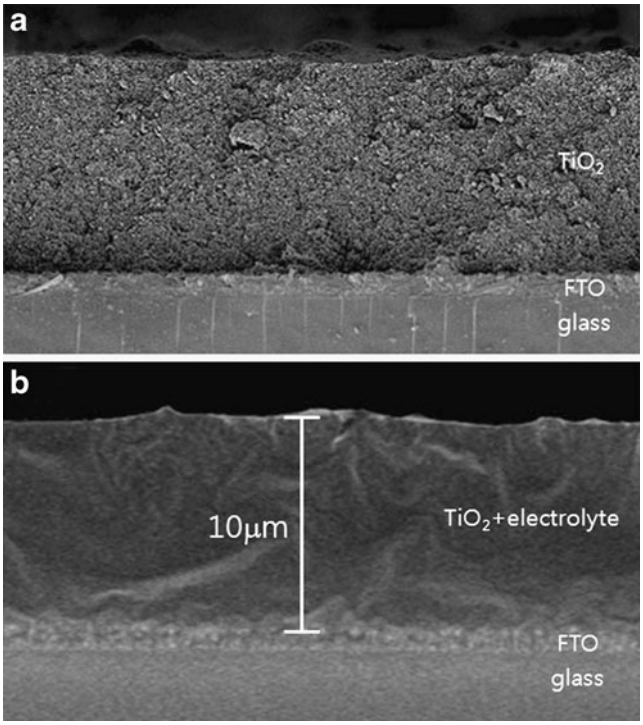

Fig. 6 Cross-sectional FE-SEM images of mesoporous TiO_2 films **a** before and **b** after casting of PEBII–POEM/MPII electrolyte

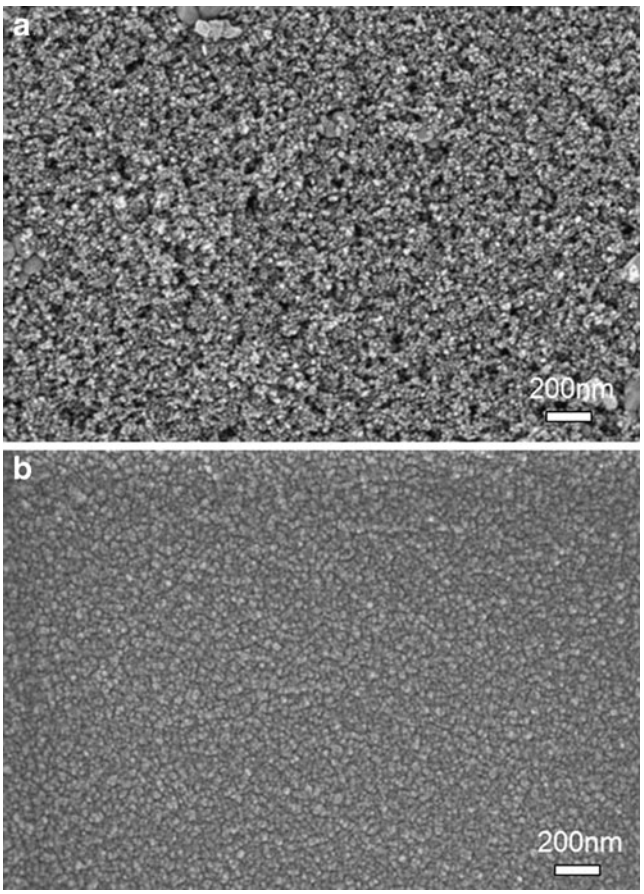

Fig. 5 Surface FE-SEM images of mesoporous TiO_2 films **a** before and **b** after casting of PEBII–POEM/MPII electrolyte

DSSCs were fabricated with four different kinds of polymer electrolytes, i.e., PEBII, PEBII–POEM, PEBII/MPII, and PEBII–POEM/MPII. The *J–V* and EIS curves were measured at 100 mW/cm^2, as shown in Figs. 7 and 8. The DSSC performances including V_{oc}, J_{sc}, FF, and η, and EIS parameters such as R_s, R_1, R_2, and W_s are summarized in Table 1, where R_s, R_1, R_2, and W_s represent the ohmic series resistance, the charge transfer resistance at the counter electrode/electrolyte, the charge resistance at the photoelectrode/electrolyte interface and the Warburg diffusion resistance in the electrolyte, respectively. The DSSC with PEBII

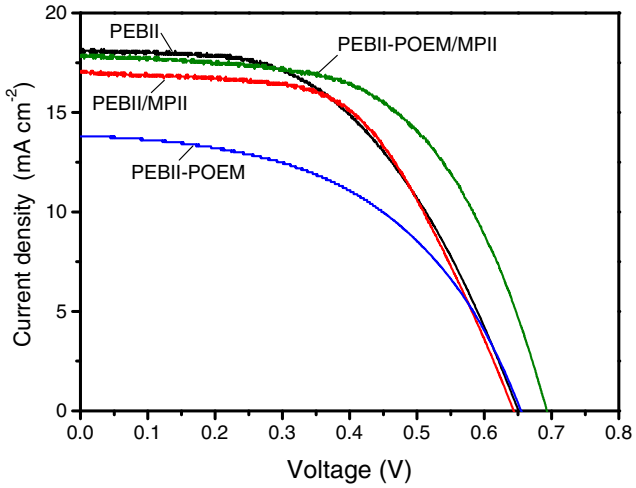

Fig. 7 Current density–voltage curves of DSSCs fabricated with PEBII, PEBII–POEM, PEBII/MPII, and PEBII–POEM/MPII electrolytes at 100 mW/cm^2

homopolymer (5.9 %) showed a higher efficiency than that with PEBII–POEM copolymer (4.5 %). Because the ionic conductivities of the two systems were not significantly different from each other, the higher efficiency of PEBII is probably due to a higher concentration of I^- ions. This indicates that ion concentration in the polymer electrolyte is a decisive factor for the performance of I_2-free DSSCs. Upon the introduction of MPII into PEBII, both J_{sc} and V_{oc} values only slightly changed, leading to a marginal change in cell efficiency (5.8 %). The interfacial resistances were also not significantly changed with the addition of MPII into PEBII. Interestingly, however, the energy conversion efficiency of the PEBII–POEM-based DSSC was significantly

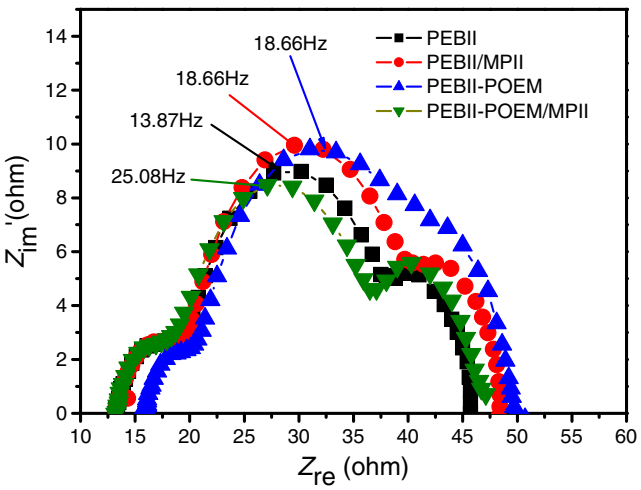

Fig. 8 Nyquist plots of DSSCs fabricated with PEBII, PEBII–POEM, PEBII/MPII, and PEBII–POEM/MPII electrolytes at 100 mW/cm^2

Table 1 DSSC performance and EIS parameters of DSSCs fabricated with four different polymer electrolytes at 100 mW/cm^2

Electrolyte	V_{oc} (mV)	J_{sc} (mA/cm^2)	FF	η (%)	R_s (Ω)	R_1 (Ω)	R_2 (Ω)	W_s (Ω)
PEBII	0.64	18.1	0.51	5.9	13.2	6.0	18.8	8.1
PEBII/MPII	0.63	17.0	0.54	5.8	13.2	6.0	21.2	8.7
PEBII–POEM	0.66	13.8	0.50	4.5	15.9	5.1	22.3	8.9
PEBII–POEM/MPII	0.69	17.8	0.57	7.0	13.8	5.0	18.7	8.1

improved up to 7.0 % by the addition of MPII. The improved efficiency is mostly due to the decreased resistances, particularly R_2 and W_s, at the photoelectrode/electrolyte interface and in the electrolyte, as characterized by EIS analysis. ^{1}H NMR analysis reveals that the weight ratio of PEBII–POEM graft copolymer is PEBII–POEM = 48:52, which corresponds to approximately 60:50 mole ratio. Because the concentration of MPII was fixed at 30 wt% with respect to the polymer, the mole ratio of PEBII/MPII–POEM is 72:28, representing that I^- concentration was increased from 60 to 72 mol% upon the introduction of MPII. Thus, MPII plays a pivotal role in increasing I^- ion concentration in PEBII–POEM, resulting in an improvement in energy conversion efficiency in DSSCs. The obtained efficiency of 7.0 % is one of the highest values for N719-based I_2-free DSSCs.

Conclusion

We synthesized a new type of random copolymer consisting of PEBII chains containing iodine ions and amorphous rubbery POEM chains having good compatibility with the hydrophilic ionic liquids. The copolymer synthesis was confirmed using FT-IR, ^{1}H NMR, UV-visible spectroscopy, and DSC. The ionic conductivities between PEBII (2.0×10^{-4} S/cm at 25 °C) and PEBII–POEM (2.2×10^{-4} S/cm) were not significantly different from each other, but the I_2-free DSSC efficiency of PEBII (5.9 % at 100 mW/cm^2) was larger than that of PEBII–POEM (4.5 %). These results indicate that ion concentration in the polymer electrolyte is a decisive factor in determining the performance of I_2-free DSSCs. Interestingly, however, the DSSC efficiency of PEBII–POEM copolymer was significantly improved up to 7.0 % by the introduction of MPII due to decreased resistances including R_2 and W_s. Thus, MPII plays an important role in increasing I^- ion concentration in PEBII–POEM, resulting in improvement of DSSC performance. The polymerized ionic liquid electrolytes deeply penetrated the TiO_2 nanopores, resulting in improved interfacial contact between electrode and electrolyte, as revealed by FE-SEM and EIS analysis.

Acknowledgments This work was supported by the Ministry of Knowledge Economy through the Human Resources Development of the Korea Institute of Energy Technology Evaluation and Planning (KETEP) (20104010100500) and by the New & Renewable Energy R&D program (2009T100100606). This work was also supported by the Ministry of Knowledge Economy (MKE) and Korea Institute for Advancement in Technology (KIAT) through the Workforce Development Program in Strategic Technology.

References

1. O'Regan B, Graetzel M (1999) Nature 353:737–739
2. Kubo W, Kitamura T, Hanabusa K, Wada Y, Yanagida S (2002) Chem Commun 2:374–375
3. Zhang DW, Li XD, Chen S, Tao F, Sun Z, Yin XJ, Huang XM (2010) J Solid State Electrochem 14:1541–1546
4. Tai Q, Chen B, Guo F, Xu S, Hu H, Sebo B, Zhao XZ (2011) ACS Nano 5:3795–3799
5. Bandara TMWJ, Dissanayake MAKL, Ileperuma OA, Varaprathan K, Vignarooban K, Mellander BE (2008) J Solid State Electrochem 12:913–917
6. Yang H, Ileperuma OA, Shimomura M, Murakami K (2009) Sol Energy Mater Sol Cells 93:1083–1086
7. Anandan S, Pitchumani S, Muthuraaman B, Maruthamuthu P (2006) Sol Energy Mater Sol Cells 90:1715–1720
8. Ganesan S, Muthuraaman B, Mathew V, Madhavan J, Maruthamuthu P, Suthanthiraraj SA (2008) Sol Energy Mater Sol Cells 92:1718–1722
9. Wang G, Wang L, Zhuo S, Fang S, Lin Y (2011) Chem Commun 47:2700–2702
10. Lee CP, Chen PY, Vittala R, Ho KC (2010) J Mater Chem 20:2356–2361
11. Xia JB, Masaki N, Lira-Cantu N, Kim Y, Jiang KJ, Yanagida S (2008) J Am Chem Soc 130:1258–1263
12. Jiang KJ, Manseki K, Yu YH, Masaki N, Suzuki K, Song YL, Yanagida S (2009) Adv Funct Mater 19:2481–2485
13. Liu X, Zhang W, Uchida S, Cai L, Liu B, Ramakrishna S (2010) Adv Mater 22:E150–E155
14. Fang Y, Xiang W, Zhou X, Lin Y, Fang S (2011) Electrochem Commun 13:60–63
15. Yanagida S, Yu Y, Manseki K (2009) Acc Chem Res 42:1827–1838
16. Docampo P, Guldin S, Stefik M, Tiwana P, Orilall MC, Hüttner S, Sai H, Wiesner U, Steiner U, Snaith HJ (2010) Adv Funct Mater 20:1787–1796
17. Crossland EJW, Nedelcu M, Ducati C, Ludwigs S, Hillmyer MA, Steiner U, Snaith HJ (2009) Nano Letters 9:2813–2819
18. Koh JK, Kim JH, Kim BG, Kim JH, Kim E (2011) Adv Mater 23:1641–1646
19. Chi WS, Koh JK, Ahn SH, Shin JS, Ahn HJ, Ryu DY, Kim JH (2011) Electrochem Commun 13:1349–1352
20. Ahn SH, Koh JH, Seo JA, Kim JH (2010) Chem Commun 46:1935–1937
21. Ahn SH, Park JT, Koh JK, Roh DK, Kim JH (2011) Chem Commun 47:5882–5884
22. Celik SU, Bozkurt A (2008) Eur Polym J 44:213–218
23. Kumar A, Deka M, Banerjee S (2010) Solid State Ionics 181:609–615
24. Noto VD, Vittadello M, Yoshida K, Lavina S, Negro E, Furukawa T (2011) Electrochim Acta 57:192–200
25. Clément S, Tizit A, Desbief S, Mehdi A, Winter JD, Gerbaux P, Lazzaroni R, Boury B (2011) J Mater Chem 21:2733–2739